RSC Advances

Cite this: *RSC Advances*, 2012, **2**, 2240–2243

www.rsc.org/advances

COMMUNICATION

Electrochemical synthesis of leaf-like CuO mesocrystals and their lithium storage properties†

Minwei Xu, Fei Wang, Bingjun Ding, Xiaoping Song and Jixiang Fang*

Received 17th November 2011, Accepted 3rd January 2012
DOI: 10.1039/c2ra01119k

We have developed an electrochemical approach for the synthesis of leaf-like CuO mesocrystals. The oriented attachment mechanism is responsible for the formation of CuO mesocrystals. As anode materials for lithium ion batteries, the high reversible capacity and enhanced cycle performance were demonstrated.

Mesocrystals were recently defined by Cölfen *et al.*, as the oriented superstructures that are built up from individual nanocrystals *via* the alignment in common crystallographic orientations.[1] Different from single crystals or superlattices, mesocrystals usually reveal the intrinsic features of rough surfaces, high porosity, single-crystalline structures and complex morphology. Hence, these dimensional and structural characteristics of mesocrystals endow them with a wide range of potential applications in catalysis, sensing, energy storage *etc.*[2] Over the past few years, mesocrystals have attracted considerable interest and various mesocrystal systems, such as metal oxide,[3] calcium carbonate,[4] metal sulfid[5] and noble metal[6] have been achieved. However, the artificial synthesis of mesocrystals *via* the oriented attachment mechanism,[7] by assembling low-dimensional building blocks, remains a great challenge. Moreover, the novel physical and chemical properties arising from the mesosuperstructures need to be addressed and their potential application as a functional material is still largely unexploited.

As an important p-type semiconductor with a narrow band gap of 1.2 eV, cupric oxide (CuO) has been extensively studied owing to its potential application in sensors, catalysts and lithium ion batteries.[8] It is well accepted that the morphology and size of CuO are important elements in determining its physical and chemical properties for the above applications. Hence, many recent efforts have been directed toward the synthesis of CuO nanostructures with diverse morphologies such as ribbons, platelets, spheres, flowers, hollow structures and dandelion-like architectures.[9] However, there are only a few reports which focus on the synthesis of CuO mesocrystals.[10] Very recently, Qi *et al.* reported the synthesis of anatase TiO_2 mesocrystals and their improved lithium storage performance.[11] To the best of our knowledge, this is the first report which focuses on the mesocrystal anode for lithium ion batteries. The introduction of mesocrystals opens a new way to improve the electrochemical performance of anode materials.

In this communication, we report an electrochemical route to synthesize leaf-like CuO mesocrystals without using any surfactants. The as-synthesized CuO nanoleaves are found to be built up from CuO nanoparticles, which share a similar crystallographic orientation. The oriented attachment mechanism is responsible for the formation of leaf-like CuO. The electrochemical properties of the CuO mesocrystals as anode material for lithium ion batteries are investigated (see ESI for experimental details†). High reversible capacity and good cycle performance are demonstrated. The improved electrochemical performance could be attributed to the unique feature of the CuO mesocrystals.

The synthesis of the CuO mesocrystals was carried out in a one-compartment cell by use of a potentiostat (Fig. S1†). Copper foils (5 mm × 30 mm) were used as the working electrode and counter electrode. The electrolyte was an aqueous solution of $NaNO_3$ (100 mM). The CuO mesocrystals were electrochemically grown at a constant voltage of 3 V for about 200 s at 70 °C. The distance between the two electrodes was kept at about 25 mm. The moderate magnetic stirring was applied throughout. The precipitates obtained in solution were harvested by centrifugation and dried at 70 °C.

Fig. 1 shows the morphologies and TEM images of the as-prepared CuO mesocrystals. The low-magnification TEM images (Fig. 1a) reveal that the mesocrystals could be produced in large-scale and have a uniform size distribution. The CuO mesocrystals display the 2D leaf-like morphology, which looks like the bamboo leaves. The width of the CuO nanoleaves is about 50 nm and the length is estimated to be about several hundred nanometres. Moreover, these CuO nanoleaves present an extremely thin thickness, which would be potentially significant for electrochemical performance. The high-magnification TEM image of individual CuO nanoleaves is presented in Fig. 1b. Interestingly, It is found that each CuO nanoleaf is composed of many small particles. The assembly of the nanoparticles causes the obtained CuO nanoleaves to exhibit the rough surface.

To further confirm the single crystal nature for the CuO mesocrystals, The obtained CuO nanoleaves were structurally characterized by TEM. Fig. 1c and d show the TEM image of an individual CuO nanoleaf and the corresponding SAED pattern. It is found that the SAED pattern shows the individual diffraction spots, demonstrating the single crystal nature for the leaf-like CuO. Moreover, Fig. 1e shows the HRTEM image of one CuO nanoleaf originating from the marked areas in Fig. 1c. A clear and continuous

MOE Key Laboratory for Nonequilibrium Synthesis and Modulation of Condensed Matter, School of Science, Xi'an Jiaotong University, Shann Xi, 710049, P. R. China. E-mail: jxfang@mail.xjtu.edu.cn; Fax: +86 29 82667872; Tel: +86 29 82665995

† Electronic supplementary information (ESI) available. See DOI: 10.1039/c2ra01119k

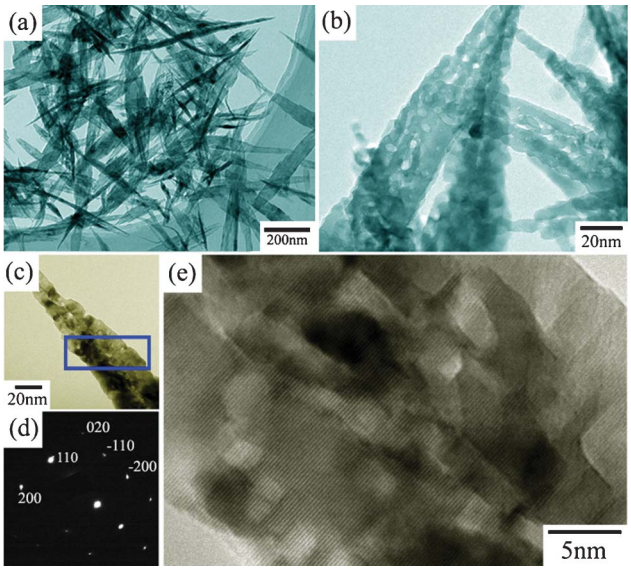

Fig. 1 TEM images of the leaf-like CuO mesocrystals in (a) low, (b) high magnification. (c) TEM image, (d) SAED patten and (e) HRTEM image of an individual CuO nanoleaf.

lattice-fringe means that the CuO nanoleaves have the same crystallographic orientation (like a single crystal). Hence, it could be concluded that the primary particles are orderly attached with each other. The parallelism of the lattice-fringes indicates that each attached nanoparticle shares the same crystallographic orientation. An added CuO nanoleaf is also shown in Fig. S2,† in which we can confirm that the obtained CuO nanoleaves are formed *via* the assembly of the nanoparticles. The insets of Fig. S2c† present the fast Fourier transform (FFT) patterns, which correspond to the respective marked areas. It is found that the FFT patterns originating from the marked areas are similar, implying that the nanocrystals within the leaf-like CuO share the same crystallographic orientation. These results show the obvious evidence that the CuO mesocrystals are formed through the oriented attachment of small nanocrystals.

The possible reaction process for the leaf-like CuO mesocrystals could be described by the formulas as follows:

$$\text{Anode: } Cu(s) \rightarrow Cu^{2+}(aq) + 2\,e^{-} \quad (1)$$

$$\text{Cathode: } 2\,H^{+}(aq) + 2\,e^{-} \rightarrow H_2\uparrow \quad (2)$$

$$\text{Solution: } Cu^{2+}(aq) + 2\,OH^{-}(aq) \rightarrow CuO(s) + H_2O \quad (3)$$

Firstly, Cu^{2+} was formed in the solution due to anodization of the copper foil. Meanwhile, the releasing of H_2 could be observed at the cathode surface. Then, the Cu^{2+} combined with OH^{-} to form $Cu(OH)_2$. In fact, the as-formed $Cu(OH)_2$ was not stable at high temperatures and tended to break down to CuO and H_2O.[12] Finally, the obtained CuO nanocrystals were self-assembled with each other to form the CuO nanostructure. Accordingly, the possible growth mechanism for the formation of the leaf-like CuO mesocrystals was proposed and schematically illustrated in Fig. 2. At the early stage, CuO nanoparticles were formed due to the dehydration of $Cu(OH)_2$. Subsequently, the CuO nanoparticles, serving as the building blocks, self-assemble along the identical direction. With the oriented

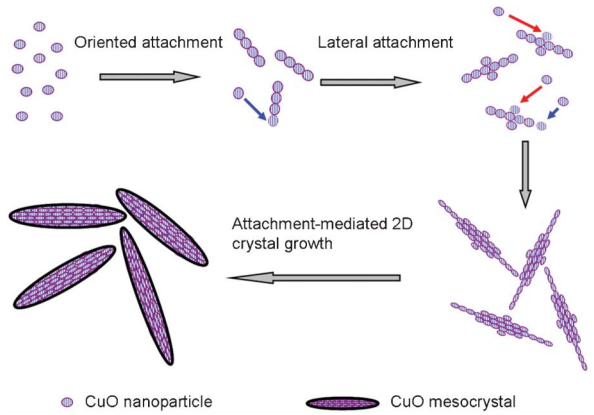

Fig. 2 Schematic illustration for the formation of leaf-like CuO mesocrystals.

attachment processes continuing, some lateral attachments of CuO nanoparticles along some side defects appeared, which were accompanied with a slowly growth along the width direction. Actually, the growth rate *via* the oriented attachment along the length and width direction was much different and hence the leaf-like CuO architectures were obtained finally. Therefore, the formation of the CuO mesocrystal is kinetic-controlled. However, the driving forces for the oriented attachment of CuO nanoparticles remains a myth to materials chemists. Several factors, including electrical and dipolar fields,[13] van der Waals forces, and hydrogen bonds may have various effects on the self-assembly.[14] More work should be done to investigate the details of the self-assembly mechanism.

XRD is used to study the phase purity of the final CuO mesocrystals, and the pattern is shown in Fig. 3a. No impurity peaks are observed. All peaks in the diffractogram are in good agreement with the tenorite phase of CuO with a monoclinic structure (JCPDS 05-0661). The leaf-like CuO mesocrystals are further characterized by nitrogen adsorption and desorption at 77 K. The N_2 adsorption and desorption isotherms and corresponding pore size distribution are shown in Fig. 3b. It is found that the leaf-like CuO exhibits a BET surface area of 23.1 $m^2\ g^{-1}$.

Recently, CuO has attracted considerable interest as a promising anode material for lithium ion batteries due to its high theoretic capacity of 670 mAh g^{-1}. However, the severe volume expansion/contraction associated with Li^{+} insertion and extraction processes causes the pulverization of the electrode, hence results in a rapid deterioration in capacity.[15] To overcome the drawback of poor cycle performance, it is suggested that the CuO electrodes should be in a nanoscaled frame.[16] Motivated by the unique architecture of the leaf-like CuO mesocrystals, the lithium storage properties of CuO

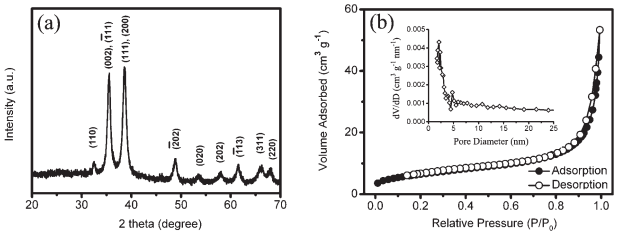

Fig. 3 (a) XRD partten and (b) N_2 adsorption and desorption isotherms for leaf-like CuO mesocrystals.

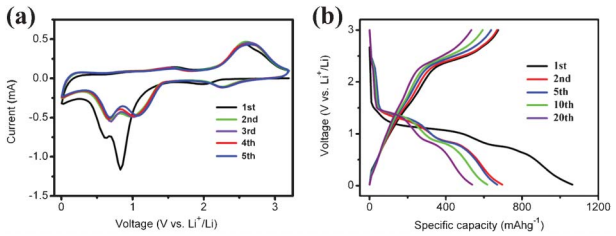

Fig. 4 (a) The first five cyclic voltammogram curves and (b) the typical charge–discharge profiles for leaf-like CuO mesocrystals.

mesocrystals were investigated. For comparison, another CuO sample is synthesized *via* an ammonia-evaporation-induced method[17] (detailed synthesis process are given in the ESI†). At the same temperature, the evaporation of ammonia induces the formation of CuO nanoparticles in the solution. However, the CuO microflakes are obtained finally (as shown in Fig. S3†). Fig. 4a shows the cyclic voltammogram (CV) curves of CuO mesocrystals at a scan rate of 0.2 mV s^{-1}. During the first cathodic scan, three peaks near 2.0 V, 0.8 V and 0.6 V can be observed. Compared to the initial cycle, a decrease of peak intensity and a shift of the potential to the positive direction are indicated in the subsequent cycles. These cathodic peaks correspond to a multistep electrochemical reaction, which is generally attributed to the solid–solution process with the formation of an intermediate phase, the reductive reaction from CuO to Cu_2O and further decomposition to Cu and Li_2O, respectively.[18] In the anodic scans, one peak in the range of 2.3 V–2.9 V is recorded, which are ascribed to the partial formation of Cu_2O and the oxidation of Cu_2O to CuO. The electrochemical reaction of Li with CuO can be expressed as follows:[19]

$$CuO + 2\ Li^+ + 2\ e^- \leftrightarrow Li_2O + Cu \quad (4)$$

The discharge–charge curves of the CuO nanoleaves are displayed in Fig. 4b, while Fig. S4† shows the discharge–charge curves for CuO microflakes. The discharge–charge behaviors and the curve plateaus are corresponding well with the cathodic and anodic peaks in Fig. 4a. However, the CuO microflakes exhibit the fast fade of capacity. Usually, the Li-driven formation of nanoscale Cu dispersed in a Li_2O matrix goes with a series of irreversible reactions during the first discharge process (*e.g.*, decomposition of electrolyte and the formation of SEI films), which results in an initial irreversible capacity and low coulombic efficiency.[20] Herein, from the cycle performance of the CuO mesocrystal as shown in Fig. 5, it can be seen that the CuO mesocrystals exhibit a high initial discharge capacity of 1063 mAh g^{-1} and a reversible capacity of 674 mAh g^{-1}, which is close to the theoretic capacity. Then, the electrode demonstrates a slow capacity fading and achieves a stable capacity above 500 mAh g^{-1} over 30 cycles. Except for the first cycle, the coulombic efficiency steadily kept higher than 96%. In contrast, the specific capacity of the CuO microflakes deteriorates quickly. The reversible capacity is less than 200 mAh g^{-1} after 30 cycles. As compared to the CuO microflakes, the leaf-like CuO mesocrystal exhibits a much better cycle performance. The improved performance may be attributed to the unique feature of the CuO mesocrystal. On the one hand, the extremely thin thickness of the CuO mesocrystal can accommodate the influence of the volume change during the lithiation/delithiation processes, which generates

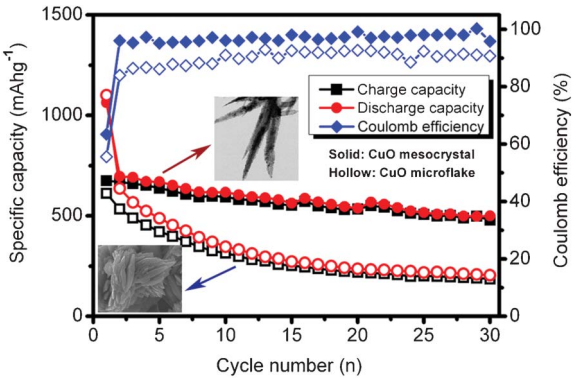

Fig. 5 The cycle performance of the leaf-like CuO mesocrystal and CuO microflake.

good capacity retention. On the other hand, the high retention of CuO mesocrystals may be attributed to the stability of the single-crystalline domains.[21] The high capacity as well as the enhanced cycle performance demonstrated that the leaf-like mesostructure is beneficial for improving the electrochemical performances of CuO anodes.

In summary, we report the electrochemical synthesis of leaf-like CuO mesocrystals. It is interesting to find that nearly all the primary particles share a similar orientation. The electrical field should play an important role in the assembly of nanoparticles. As anode materials for lithium ion batteries, the obtained CuO mesocrystals exhibit high specific capability and good cycle performance, which can be attributed to the novel feature of the CuO mesocrystals.

Acknowledgements

We thank the supports from the National Natural Science Foundation of China (nos. 51171139, 50901056), Tengfei Talent Project of Xi'an Jiaotong University, the New Century Excellent Talents in University (NCET) and the Fundamental Research Funds for the Central Universities (No. 08142008).

References

1 H. Cölfen and M. Antonietti, *Angew. Chem., Int. Ed.*, 2005, **44**, 5576.
2 (*a*) R. Q. Song and H. Cölfen, *Adv. Mater.*, 2010, **22**, 1301; (*b*) J. X. Fang, B. J. Ding and H. Gleiter, *Chem. Soc. Rev.*, 2011, **40**, 5347.
3 (*a*) J. X. Fang, P. M. Leufkea, R. Kruka, D. Wang, T. Scherera and H. Hahn, *Nano Today*, 2010, **5**, 175; (*b*) D. Wang, J. Li, X. Cao, G. S. Pang and S. H. Feng, *Chem. Commun.*, 2010, **46**, 7718.
4 T. X. Wang, H. Cölfen and M. Antonietti, *J. Am. Chem. Soc.*, 2005, **127**, 3246.
5 (*a*) N. Wang, X. Cao, L. Guo, S. H. Yang and Z. Y. Wu, *ACS Nano*, 2008, **2**, 184; (*b*) C. C. Kang, C. W. Lai, H. C. Peng, J. J. Shyue and P. T. Chou, *ACS Nano*, 2008, **2**, 750.
6 (*a*) J. X. Fang, S. Y. Du, S. Lebedkin, Z. Y. Li, R. Kruk, M. Kappes and H. Hahn, *Nano Lett.*, 2010, **10**, 5006; (*b*) J. X. Fang, B. J. Ding and X. P. Song, *Cryst. Growth Des.*, 2008, **8**, 3616; (*c*) J. X. Fang, B. J. Ding, X. P. Song and Y. Han, *Appl. Phys. Lett.*, 2008, **92**, 173120; (*d*) J. X. Fang, B. J. Ding and X. P. Song, *Appl. Phys. Lett.*, 2007, **91**, 083108.
7 (*a*) M. Niederberger and H. Cölfen, *Phys. Chem. Chem. Phys.*, 2006, **8**, 3271; (*b*) Q. Zhang, S. J. Liu and S. H. Yu, *J. Mater. Chem.*, 2009, **19**, 191; (*c*) D. P. Volanti, M. O. Orlandi, J. Andres and E. Longo, *CrystEngComm*, 2010, **12**, 1696.
8 (*a*) F. Teng, W. Q. Yao, Y. F. Zheng, Y. T. Ma, Y. Teng, T. G. Xu, S. H. Liang and Y. F. Zhu, *Sens. Actuators, B*, 2008, **134**, 761; (*b*) E. Reitz, W. Z. Jia, M. Gentile, Y. Wang and Y. Lei, *Electroanalysis*, 2008, **20**, 2482; (*c*) J. Y. Kim, J. C. Park, H. Kang, H. Song and K. H. Park, *Chem.*

Commun., 2010, **46**, 439; (*d*) P. Poizot, S. Laruelle, S. Grugeon, L. Dupont and J. M. Tarascon, *Nature*, 2000, **407**, 496.
9 (*a*) X. L. Gou, G. X. Wang, J. Yang, J. Park and D. Wexler, *J. Mater. Chem.*, 2008, **18**, 965; (*b*) T. Soejima, H. Yagyu, N. Kimizuka and S. Ito, *RSC Adv.*, 2011, **1**, 187; (*c*) G. F. Zou, H. Li, D. W. Zhang, K. Xiong, C. Dong and Y. T. Qian, *J. Phys. Chem. B*, 2006, **110**, 1632; (*d*) J. Liu, X. T. Huang, Y. Y. Li, K. M. Sulieman, X. He and F. L. Sun, *J. Mater. Chem.*, 2006, **16**, 4427; (*e*) J. C. Park, J. Kim, H. Kwon and H. Song, *Adv. Mater.*, 2009, **21**, 803; (*f*) B. Liu and H. C. Zeng, *J. Am. Chem. Soc.*, 2004, **126**, 8124.
10 (*a*) H. L. Xu, W. Z. Wang, W. Zhu, L. Zhou and M. L. Ruan, *Cryst. Growth Des.*, 2007, **7**, 2720; (*b*) J. P. Liu, X. T. Huang, Y. Y. Li, K. M. Sulieman, X. He and F. L. Sun, *J. Mater. Chem.*, 2006, **16**, 4427; (*c*) J. P. Liu, X. T. Huang, Y. Y. Li, K. M. Sulieman, X. He and F. L. Sun, *Cryst. Growth Des.*, 2006, **6**, 1690.
11 J. F. Ye, W. Liu, J. G. Cai, S. Chen, X. W. Zhao, H. H. Zhou and L. M. Qi, *J. Am. Chem. Soc.*, 2011, **133**, 933.
12 Y. H. Ni, H. Li, L. N. Jin and J. M. Hong, *Cryst. Growth Des.*, 2009, **9**, 3868.
13 (*a*) X. Z. Lin, P. Liu, J. M. Yu and G. W. Yang, *J. Phys. Chem. C*, 2009, **113**, 17543; (*b*) Z. Y. Tang, N. A. Kotov and M. Giersig, *Science*, 2002, **297**, 237.
14 L. S. Zhong, J. S. Hu, H. P. Liang, A. M. Cao, W. G. Song and L. J. Wan, *Adv. Mater.*, 2006, **18**, 2426.
15 (*a*) S. Y. Gao, S. X. Yang, J. Shu, S. X. Zhang, Z. D. Li and K. Jiang, *J. Phys. Chem. C*, 2008, **112**, 19324; (*b*) S. F. Zheng, J. S. Hu, L.S. Zhong, W. G. Song, L. J. Wan and Y. G. Guo, *Chem. Mater.*, 2008, **20**, 3617.
16 J. Y. Xiang, J. P. Tu, L. Zhang, Y. Zhou, X. L. Wang and S. J. Shi, *J. Power Sources*, 2010, **195**, 313.
17 (*a*) Y. G. Li, B. Tan and Y. Y. Wu, *Chem. Mater.*, 2008, **20**, 567; (*b*) Y. G. Li, B. Tan and Y. Y. Wu, *J. Am. Chem. Soc.*, 2006, **128**, 14258.
18 A. Debart, L. Dupont, P. Poizot, J. B. Leriche and J. M. Tarascon, *J. Electrochem. Soc.*, 2001, **148**, A1266.
19 (*a*) J. Y. Xiang, J. P. Tu, Y. F. Yuan, X. H. Huang, Y. Zhou and L. Zhang, *Electrochem. Commun.*, 2009, **11**, 262; (*b*) J. Y. Xiang, J. P. Tu, L. Zhang, Y. Zhou, X. L. Wang and S. J. Shi, *Electrochim. Acta*, 2010, **55**, 1820.
20 S. Laruelle, S. Grugeon, P. Poizot, M. Dolle, L. Dupont and J. M. Tarascon, *J. Electrochem. Soc.*, 2002, **149**, A627.
21 J. C. Park, J. Kim, H. Kwon and H. Song, *Adv. Mater.*, 2008, **20**, 1.